FINAL SCIENTIFIC REPORT

TITLE OF RESEARCH:

NAGW 588

Solar Flare X-ray Polarimetry

PERIOD OF RESEARCH:

April 1, 1984 to September 30, 1986

SUBMITTED TO:

National Aeronautics and Space Administration Headquarters
Solar and Heliosperic Physics Office
Washington, DC 20546

PREPARED BY:

Department of Physics
University of California
Irvine, Claifornia 92717

and

Columbia Astrophysics Laboratory
Departments of Astronomy and Physics
Columbia University
538 West 120th Street
New York, NY 10027

PRINCIPAL INVESTIGATOR:

G. A. Chanan
Associate Professor of Physics
University of California, Irvine

CO-INVESTIGATOR:

R. Novick
Professor of Physics
Columbia University

October 1986

I. Introduction

As described in the original proposal (CAL-1529, January 1984) this grant was for the support of a preliminary design study for an instrument to be used to measure the X-ray polarization of solar flares during the maximum of next solar cycle, in or about 1991. Three specific tasks were identified for this design; these were:

1. to improve the sensitivity of the instrument over that of the OSS-1 polarimeter by a factor of 3 or 4 (at 15 keV),
2. to extend the energy range of the instrument substantially beyond 20 keV, the effective upper limit of the OSS-1 polarimeter, and
3. to demonstrate that the lithium contamination problem experienced with the OSS-1 experiment has been overcome.

We have in fact attained each of these goals. In the following we first review the motivation for high quality solar flare X-ray polarization measurements in general and for the goals 1 and 2 above in particular. We then describe the design of the proposed instrument and discuss the sensitivity and energy response. Fianlly we describe laboratory work which demonstrates that the earlier lithium contamination problem has been solved (goal 3).

II. History and Motivation

The idea that X-ray emission from solar flares might be linearly polarized and that polarization measurements could therefore provide a strong flare diagnostic was first discussed by Korchak (1967) and Elwert (1968). Subsequent theoretical investigations (Elwert and Haug 1970, 1971; Haug 1972; Brown 1972; Henoux 1975; Langer and Petrosian 1977; Bai and Ramaty 1978; Emslie and Brown 1980) have resulted in polarization predictions for a variety of models. The two broad classes of models, thermal and non-thermal, differ significantly in their polarization predictions: the thermal models predict polarizations of at most a few percent (Henoux 1975, Emslie and Brown 1980) due to scattering in the photosphere. The beamed or linear bremsstrahlung models, on the other hand predict strongly polarized emission (~10%).

The two models also predict different directivities, with the non-thermal models tending to give anistropic distributions (Elwert and Haug 1970, 1971), although the intrinsic effect is substantially reduced by photospheric backscattering (Bai and Ramaty 1978). Stereoscopic observations by Kane et al. (1980) put limits on the anistropy and tend to favor the thermal models, but are thus far not conclusive. Recent gamma ray observations from SMM show that above 300 keV more flares are observed at the limb of the solar disk than at the center (Rieger et al. 1983, Vestrand 1985). Dermer and Ramaty (1986) have attributed this effect to the beaming of electrons parallel to the surface of the sun. It is important to recognize that the observations of

photon beaming directly imply non-vanishing polarization. The beaming observations that have been made to date are purely statistical in nature. They require one to compare the photon fluxes from different solar flares; since no two flares are the same this is a very suspect procedure. Polarimetric observations would provide direct evidence for electron beaming within a particular flare without recourse to comparing data from different flares.

The pioneering observational work in solar X-ray polarimetry was done in a series of satellite experiments by Tindo and his collaborators in the Soviet Union (Tindo et al. 1972a, 1972b; Tindo, Mandel'stam, and Shuryghin 1973; Tindo, Shuryghin, and Steffen 1976). Initial results showed high levels of polarization (up to 40%), although of rather low statistical significance, and these were generally interpreted as evidence for strong beaming of the electrons. These results are shown in Figure 1 where they are compared to the theoretical calculations of Bai and Ramaty (1978). The results of the polarimeter flown by the Columbia Astrophysics Laboratory as part of the OSS-1 payload on the Space Shuttle mission STS-3 by contrast showed very low levels of polarization - no more than a few percent (Tramiel, Chanan, and Novick 1984). At the same time but independent of the observational work, Leach and Petrosian (1983) showed that the high levels of polarization in the Tindo results were difficult to understand theoretically, since the electron beam is isotropized on an energy loss timescale - an effect which substantially reduces the expected levels of polarization,

although not to zero. These latter results are also shown in Figure 1. In Figure 2 we compare the OSS-1 results to the calculations of both Bai and Ramaty and Leach and Petrosian. These results are considerably below those of Tindo and all of the theoretical results. As noted on Figure 2 one of the OSS-1 events was impulsive in nature. A subsequent comparison by Leach, Emslie, and Petrosian (1985) to the (impulsive phase) OSS-1 result and the above theoretical treatment shows that the former are consistent with several current models (see Figure 3) and that a factor of ~3 improvement in sensitivity is needed to distinguish properly among the possibilities. In addition, there is reason to expect stronger polarization effects at higher energies: although the predicted polarization curves of Leach and Petrosian (1983) are only weakly energy dependent (up to at least 100 keV), there may be a strong admixture of thermal X-rays at the energies seen by the OSS-1 instrument (5-20 keV, but predominantly below 10 deV). As Leach, Emslie, and Petrosian (1985) stress, this thermal "contamination" will tend to reduce the observed polarization, but the effect should decrease sharply with increasing energy (see also Emslie and Vlahos 1980), so that the need for higher energy observations is clear. Clearly better polarimetric observations are needed, particularly at high energies where thermal effects are unimportant. In the next section we describe a new polarimeter, designed under the current grant and intended to answer the outstanding questions regarding electron beaming and scattering in solar flares.

III. The Proposed Instrument

The previous (OSS-1) instrument (Lemen et al. 1982) exploited the polarization dependence of Thomson scattering. The targets (whose dimensions are set by the relevant scattering length) were 12 rectangular blocks of metallic lithium, monitored on two of the four sides by xenon-filled proportional counters; there were thus effectively six targets. The low energy threshold was set at ~5 keV by photoelectric losses in the lithium, the high energy cutoff by the transparency of the proportional counters at ~20 keV. We now propose to use plastic scintillator (composed mainly of carbon) in place of the lithium targets. This will raise the low energy threshold to ~10 keV. Below this energy the X-rays are largely thermal so the reduced low energy response is inconsequential. The xenon counters will in turn be replaced by sodium iodide detectors [NaI(Tℓ)]; this will extend the high energy response upward by a factor of 5 to 100 keV.

A fundamental improvement in background rejection will result from using the carbon target in the form of plastic scintillator. A sufficiently high energy photon which interacts in the target will give rise to a Compton electron whch can be detected by a photomultiplier tube which monitors the optical output of the target from below. This can then be used as a trigger for the acceptance of events in the NaI(Tℓ) detectors. Although the exact value of the Compton threshold (estimated to be ~40 keV) is somewhat uncertain, the ultimate performance of the instrument is not very sensitive to the precise value. The reason is that at energies which are low enough for the detection

of the Compton electron to be difficult, the source fluxes are high enough that the background is simply not a problem (this was in fact the case with the OSS-1 polarimeter). Conversely, at energies which are sufficiently high that good background rejection is essential (because of the low fluxes), the Compton electron will have enough energy that it will be relatively easy to detect. In fact since both target and detector events will be recorded in flight, the precise value of the Compton threshold can be chosen post-flight to optimize the polarization response.

Because the NaI(Tℓ) detectors are relatively compact, a large number of target/detector assemblies can be packed into a relatively small space. We further plan to adopt a hexagonal geometry (as opposed to the square geometry used on OSS-1); this results in an improved modulation factor which in turn results in higher sensitivity and reduced vulnerability to systematic effects. Current plans are for an array of 37 targets each surrounded by 6 detectors (the latter shared by 2 targets, except on the periphery) (see Figures 4, 5, and 6). Such an array would be 28 in. in diameter.

The photon collection efficiency of this device has been calculated by a semi-analytic approximation and is plotted in Figure 7. At 15 keV, about 16% of the incident photons are detected, compared to 11% at this energy for the OSS-1 experiment. This difference is due principally to the detectors; the xenon counters are already becoming transparent at this relatively low energy. The modulation factor for the hexagonal geometry can be shown to be approximately $3\sqrt{3}/4\pi = 0.414$ as

compared to $1/\pi = 0.318$ for a square geometry. The overall sensitivity is proportional to the square root of both the photon collection efficiency and the number of scattering targets and directly proportional to the modulation factor. The current design therefore represents an improvement in sensitivity (at 15 keV) of a factor of

$$\left(\frac{16}{11}\right)^{1/2}\left(\frac{37}{6}\right)^{1/2}\left(\frac{0.414}{0.318}\right) = 3.9$$

over the OSS-1 experiment. As noted above, in addition, the energy range has been extended upward by a factor of 5. The entire polarimeter assembly can be rotated to avoid a large number of possible systematic effects (instrumental polarization).

Sensitivity calculations for the instrument described above for 5 typical (moderate) flares are shown in Table I; the flare parameters were taken from actual observed events (Lemen 1981). Assumed integration times are 10 s in each case, consistent with the faster timescales of impulsive events. Note that sensitivities of a few percent are routinely attained up to ~100 keV energies. The number of photons detected as a function of energy is shown for these flares in Figures 8a-e.

We stress that the above design is based on laboratory tests of individual modules, on detailed computer simulations, and incorporates the heritage of several successful rocket flights as well as that of the OSS-1 experiment. The proposed polarimeter is well matched to the outstanding questions about electron beaming and scattering in solar flares.

IV. The Contamination Problem

As discussed by Tramiel, Chanan, and Novick (1984), some problems were experienced with the OSS-1 polarimeter as the result of contamination of the lithium blocks. A post-flight inspection of the experiment revealed that the contamination resulted from damage to the outermost of two plastic coatings used to protect the lithium. This damage apparently occurred during the final assembly of the instrument; two spare "witness" targets, not incorporated into the instrument, showed no such damage and no degradation. Even though the instrument under discussion here will be based on plastic scintillator (and not lithium) scattering targets, we still felt that it was essential to find a solution to the lithium contamination problem and to demonstrate its effectiveness. Two reasons for doing this are: (i) A few of the plastic targets in the new instrument may be replaced with lithium. This would substantially extend the bandwidth of the instrument. Even only two or three such targets would provide good low energy sensitivity, since the low energy fluxes are so high. (ii) There appears to be some chance that the OSS-1 instrument may be re-flown.

As a result of the STS-3 experience, shortly after the flight, we obtained beryllium housings in which the lithium targets could be encased and hermetically sealed (see Figure 9). The thickness of the beryllium is about 40 mils, small enough to have a negligible effect on the performance of the polarimeter. Since beryllium is very strong structurally (comnparable to steel), the possibility of damage during assembly is eliminated. However, it still remained for the present study

to demonstrate that we could obtain an airtight seal between the container and the stainless steel base of the scattering target. We therefore obtained six lithium scattering targets to seal in the beryllium cans. Since both lithium oxide and lithium nitride are substantially heavier than lithium metal, we were able to assess the quality of the seal simply by weighing the targets over a long period of time on a sensitive balance. For a given contaminant, it is a straightforward matter to calculate the systematic polarization caused by a given mass gain, under the worst-case assumption that the contaminant is deposited only on one side of the target. [For simplicity we assume a square geometry and uniform deposition over the side of the target in question.] The results of such a calculation are shown in Table II, where we have assumed that the weight gain is due to the nitride (identified as the contaminant in OSS-1) and the exact geometry of the OSS-1 targets has been assumed. We note that quite similar results are obtained if the contaminant is lithium oxide.

From Table II, a reasonable criterion is that the mass gain (per target) not exceed 125 mg; this gives a systematic polarization of 1% (comparable to the expected statistical errors) at 10 keV, and considerably lower values at higher energies. Since one would like the targets to last for about a year (including assembly, pre-flight calibration, flight, and post-flight calibration), the weight gain rate should not exceed 0.34 mg day^{-1}.

In July 1985 we assembled 3 lithium target/beryllium canister assemblies. Two targets, numbers 1 and 3, did not meet

the above specification, showing weight gain rates of 1.6 mg day^{-1} and 3.5 mg day^{-1} respectively (see Figure 10a and c). However, the remaining target, number 2, was considerably better than the specification, showing a nominal weight gain of only 0.076 mg day^{-1} (Figure 10b); at this rate the targets would last for well over 4 years.

Visual inspection of targets 1 and 3 readily showed that the problem was due either to insufficient trimming of some excess lithium from around the stainless steel base or to using excess glue to join the base to the housing. The result in either case was to allow the lithium to come in contact with the glue and apparently a subsequent chemical reaction affected the integrity of the glue joint.

In November of 1985 we prepared two additional target/canister assemblies similar to the first three, but we took greater care to insure that the lithium and glue could not contact each other. We also implemented some additional refinements in the assembly technique, including repairing the glove box which provided the inert (argon) atmosphere in which the assembly was done. The targets, numbers 4 and 5, assembled in this way both showed excellent seals, with weight gains comparable to those of target 4 - 0.072 mg/day and 0.113 mg/day, respectively (see Figure 10e,f). We believe that this convincingly demonstrates that we have solved the lithium contamination problem. We note that we plan to continue to monitor the target weights to determine the long-term behavior of the seals.

At the same time as targets 4 and 5 were fabricated, we

prepared a sixth target, but in an aluminum housing equipped with a vacuum/pressure gauge. The purpose of this was to determine whether there was any outgassing from the lithium; if there were, then the assembly would in effect be a pressure vessel and this could be a concern on future space flights. However, to within the accuracy of the gauge (0.2 lb in^{-2}) there has been no change in pressure over a time base of many months. We believe that this demonstrates that such assemblies would not act as pressure vessels and that they could therefore be used safely in space. Again, we will continue to monitor this target to study its long-term behavior. We note that because of the additional weight of the pressure gauge, this target would not be weighed on the fine range of our scale, and so a sensitive measure of the weight gain is not yet available, although it is consistent with zero (see Figure 10f).

In summary we have demonstrated that we have solved the lithiuim contamination problem and have in fact prepared several targets which are a factor of 4 better than the contaminant specification. We have also demonstrated that there is no pressure build-up in the sealed target assemblies and that they should therefore be safe for use in space.

REFERENCES

Bai, T., and Ramaty, R. 1978, Astrophys. J. 219, 705.

Brown, J. C. 1972, Solar Physics 26, 441.

Dermer, C. D. and Ramaty, R. 1986, Astrophys. J. 301, 962.

Elwert, G. 1968, in K. O. Kiepenheuer (ed.), "Structure and Development of Solar Active Regions," IAU Symp. 35, 444.

Elwert, G., and Haug, E. 1970, Solar Phys. 15, 234.

Elwert, G., and Haug, E. 1971, Solar Phys. 20, 413.

Emslie, A. G., and Brown, J. C. 1980, Astrophys. J. 237, 1015.

Emslie, A. G., and Vlahos, L. 1980, Astrophys. J. 242, 359.

Haug, E. 1972, Solar Physics 25, 425.

Henoux, J. C. 1975, Solar Phys. 42, 219.

Kane, S. R. et al. 1980, Astrophys. J. (Letters), 239, L85.

Korchak, A. A. 1967, Soviet Phys. Dokl. 12, 192.

Langer, S. H., and Petrosian, V. 1977, Astrophys. J. 215, 666.

Leach, J., and Petrosian, V. 1983, Astrophys. J. 269, 715.

Leach, J., Emslie, A. G., and Petrosian, V. 1985, Solar Phys., 96, 331.

Lemen, J. R. 1981, Ph.D. Thesis, Columbia University (unpublished).

Lemen, J. R., Chanan, G. A., Hughes, J. P., Laser, M. R., Novick, R., Rochwarger, I. R., Sackson, M., and Tramiel, L. J. 1982, Solar Phys. 80, 333.

Reiger, E., Reppin, C., Kanbach, G., Forrest, D. J., Chupp, E. L., and Share, G. H. 1983, in 18th International Cosmic Ray Conference (Late Papers), Bangalore, 10, 338.

Tindo, I. P., Ivanov, V. D., Mandel'stam, S. L., and Shuryghin, A. I. 1972a, Solar Phys. 24, 429.

Tindo, I. P., Ivanov, V. D., Valnicek, B., and Livshits, M. A. 1972b, Solar Phys. 27, 426.

Tindo, I. P., Mandel'stam, S. L., and Shuryghin, A. I. 1973, Solar Phys. 32, 469.

Tindo, I. P., Shuryghin, A. I., and Steffen, W. 1976, Solar Phys. 46, 219.

Tramiel, L.J., Chanan, G. A., and Novick, R. 1984, Astrophys. J. 280, 440.

Table I

Polarization Sensitivies (1σ) Predicted for Five Typical Flares

(10 second observation time)

1. Photon flux at 1 keV = 1.35×10^5 photons cm^{-2} s^{-1} kev^{-1}
   Spectral index = 3.34
   Classification = M2

Energy Range	Polarization
10-20 keV	1.25%
20-30 keV	1.70%
30-40 keV	2.69%
40-50 keV	3.89%
50-60 keV	5.40%
60-100 keV	4.25%

2. Photon flux at 1 keV = 3.60×10^7 photons cm^{-2} s^{-1} keV^{-1}
   Spectral index = 4.28
   Classification = X2

Energy Range	Polarization
10-20 keV	0.27%
20-30 keV	0.46%
30-40 keV	0.87%
40-50 keV	1.41%
50-60 keV	2.15%
60-100 keV	2.01%

3. Photon flux at 1 keV = 2.61×10^7 photons cm^{-2} s^{-1} keV^{-1}
   Spectral index = 4.66
   Classification = M3

Energy Range	Polarization
10-20 keV	0.52%
20-30 keV	1.01%
30-40 keV	2.02%
40-50 keV	3.44%
50-60 keV	5.47%
60-100 keV	5.46%

Table I (continued)

Polarization Sensitivies (1σ) Predicted for Five Typical Flares

(10 second observation time)

4. Photon flux at 1 keV = 2.49×10^{7} photons cm^{-2} s^{-1} keV^{-1}
   Spectral index = 4.36
   Classification = M3

Energy Range	Polarization
10-20 keV	0.36%
20-30 keV	0.63%
30-40 keV	1.20%
40-50 keV	1.97%
50-60 keV	3.03%
60-100 keV	2.87%

5. Photon flux at 1 keV = 2.30×10^{5} photons cm^{-2} s^{-1} keV^{-1}
   Spectral index = 3.0
   Classification = M2

Energy Range	Polarization
10-20 keV	0.60%
20-30 keV	0.75%
30-40 keV	1.12%
40-50 keV	1.55%
50-60 keV	2.09%
60-100 keV	1.74%

Table II

Theoretical Instrumental Polarization as a Function of Contaminant Mass

	m(gm)			
E(keV)	1/8	1/4	1/2	1
5	0.0823	0.165	0.328	0.650
6	0.0468	0.0936	0.187	0.373
8	0.0192	0.0384	0.0769	0.154
10	0.00961	0.0192	0.0384	0.0769
15	0.00280	0.00560	0.0112	0.0224
20	0.00124	0.00248	0.00495	0.00991
30	0.000495	0.000991	0.00198	0.00396

Figure Captions

Figure 1: Comparison of the polarization results of Tindo (1976) with the theoretical results of Bai and Ramaty (1978) and of Leach and Petrosian (1983). Note that the theoretical curves of Leach and Petrosian are considerably below the polarization results of Tindo.

Figure 2: Comparison of the OSS-1 (STS-3) polarization results with the calculation of Bai and Ramaty (1978) and Leach and Petrosian (1983). Note that the STS-3 results are lower than all of the theoretical predictions.

Figure 3: Comparison of the STS-3 impulsive event polarization result with theoretical predictions of Leach, Emslie, and Petrosian (1985). See the latter paper for details of the three different models indicated.

Figure 4: Basic hexagonal polarimeter configuration. Note that the scattering target consists of an active scintillator which produces a light pulse when a Compton scattering event takes place in the target. The scattered photon is recorded by one of the six NaI(Tℓ) detectors that surround the target.

Figure 5: Assembly of the scintillation targets and surrounding NaI(Tℓ) detectors.

Figure 6: Complete solar flare polarimeter consisting of 37 scintillator targets and surrounding NaI(Tℓ) detectors. The entire assembly can be rotated at 20 rpm to avoid systematic effects.

Figure 7: Photon collection efficiency for the plastic target/ NaI(Tℓ) detector polarimeter.

Figure 8 a-e: Number of photons per keV collected in 10s for the 5 flares considered in Table I. The flare normalization is A and the spectral index is α. (See Table I).

Figure 9: Beryllium housing for lithium targets.

Figure 10 a-f: Mass of lithium target assemblies as a function of time. Targets 1 and 3 are out of specification for the reason discussed in the text. Targets 2, 4, and 5 are all considerably better than contaminant specification. Target 6 is equipped with a pressure gauge which prevents its being weighed with the same accuracy as the other targets.

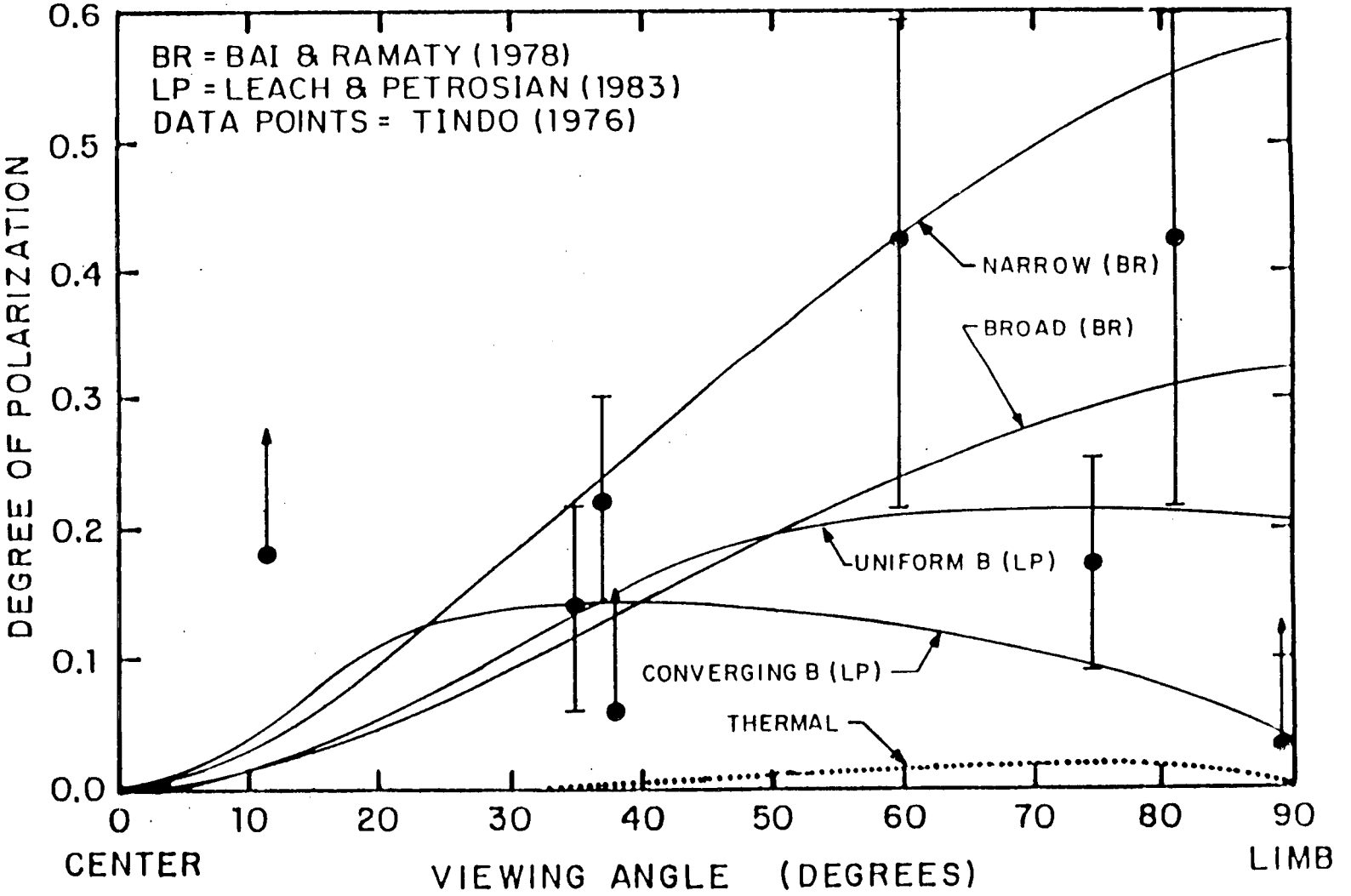
BR = BAI & RAMATY (1978)
LP = LEACH & PETROSIAN (1983)
DATA POINTS = TINDO (1976)
NARROW (BR)
BROAD (BR)
UNIFORM B (LP)
CONVERGING B (LP)
THERMAL
DEGREE OF POLARIZATION
0.0
0.1
0.2
0.3
0.4
0.5
0.6
0
10
20
30
40
50
60
70
80
90
CENTER
LIMB
VIEWING ANGLE (DEGREES)

Figure 1

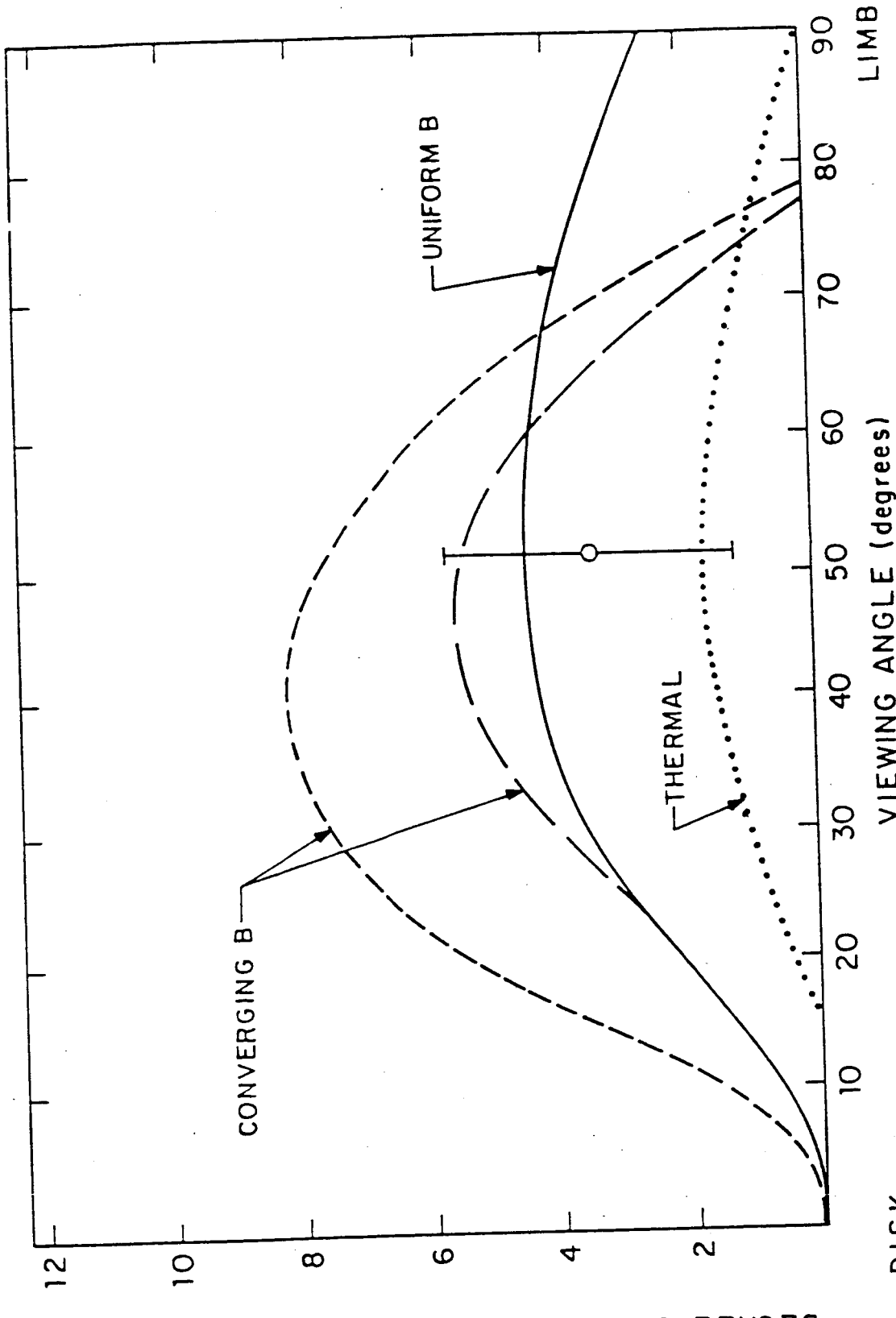

Figure 3

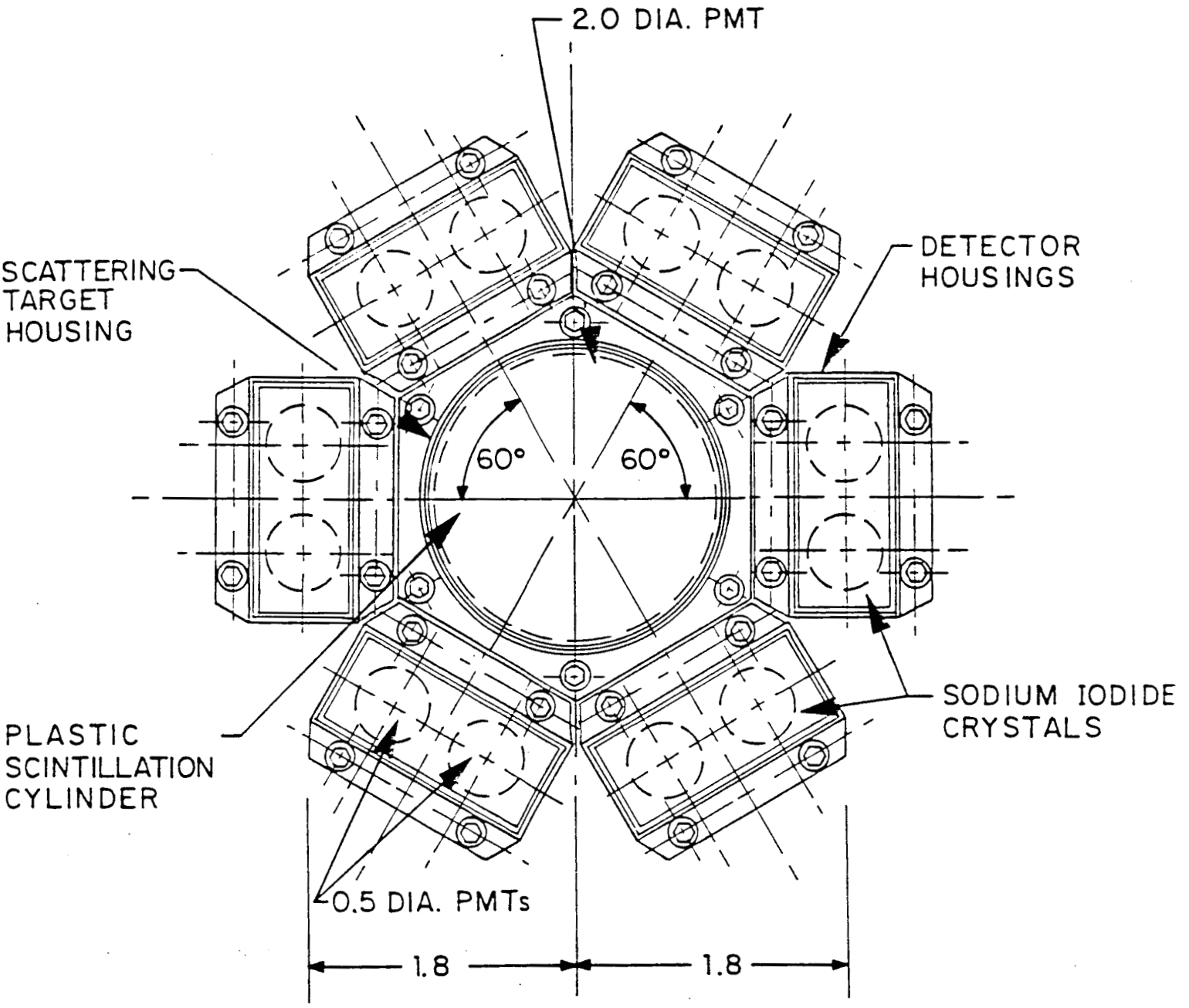

A-A-1053 JD

Figure 5

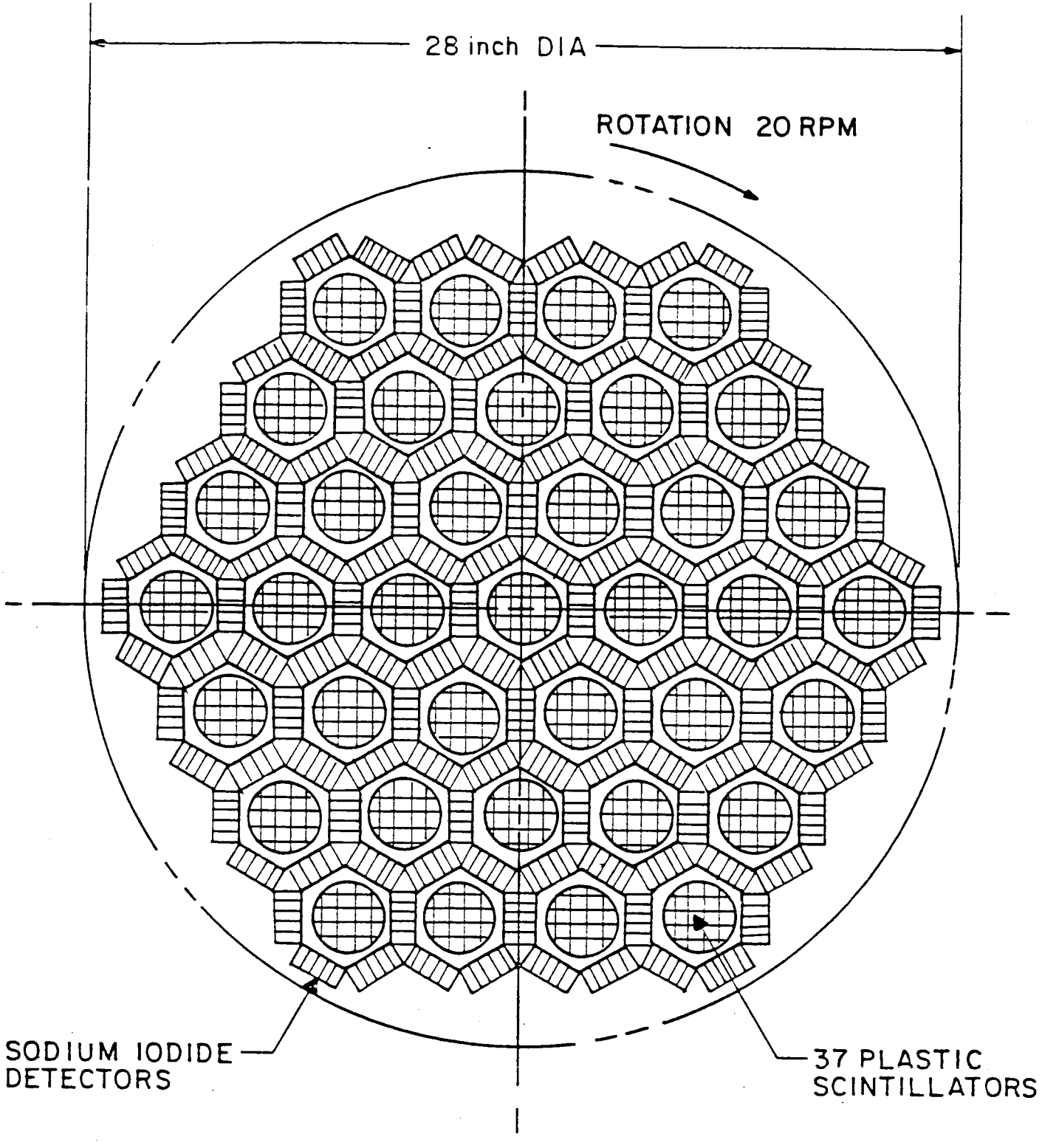
28 inch DIA
ROTATION 20 RPM
SODIUM IODIDE DETECTORS
37 PLASTIC SCINTILLATORS

Figure 6

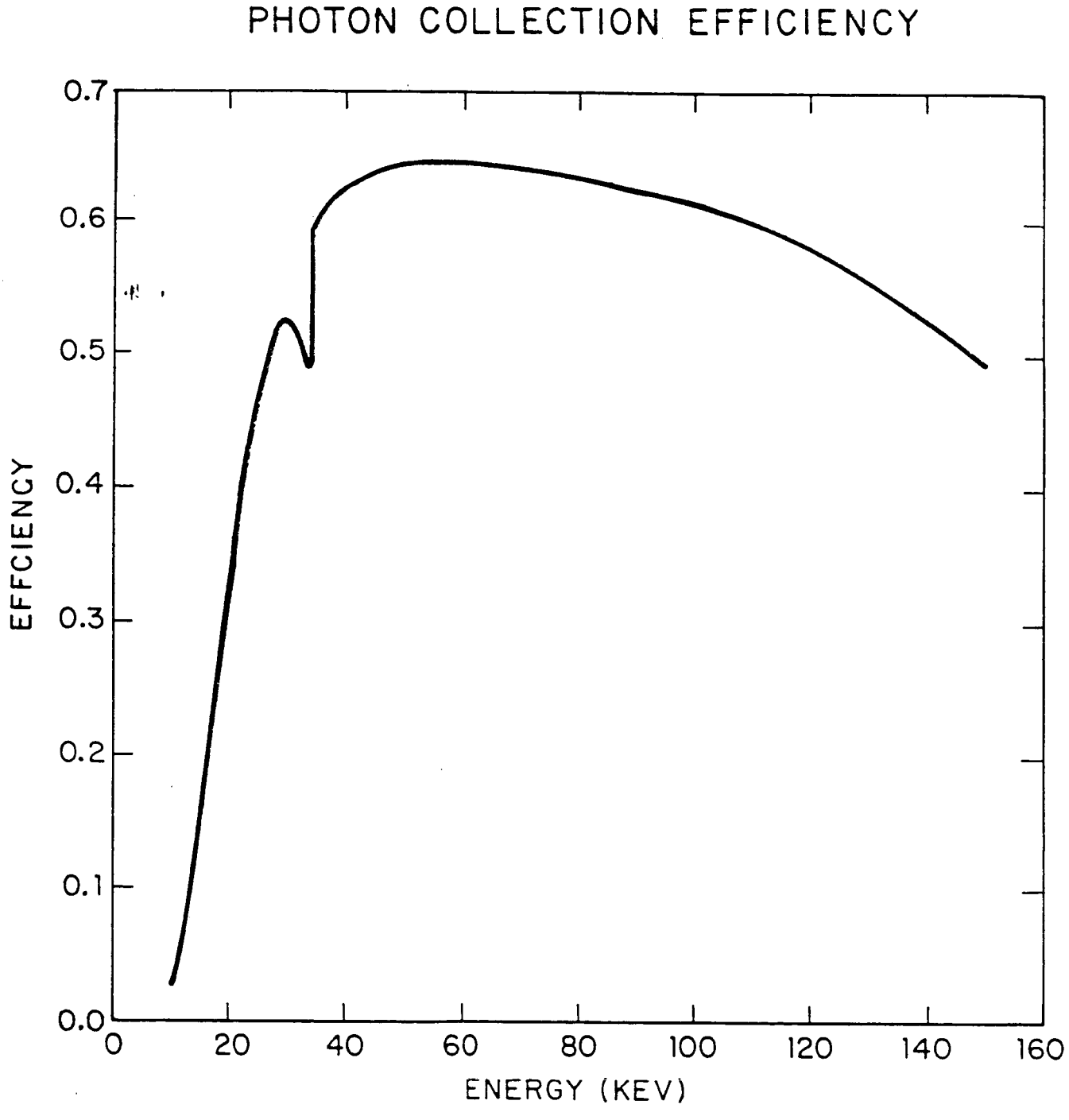
PHOTON COLLECTION EFFICIENCY
EFFCIENCY
0.0
0.1
0.2
0.3
0.4
0.5
0.6
0.7
0
20
40
60
80
100
120
140
160
ENERGY (KEV)

Figure 7

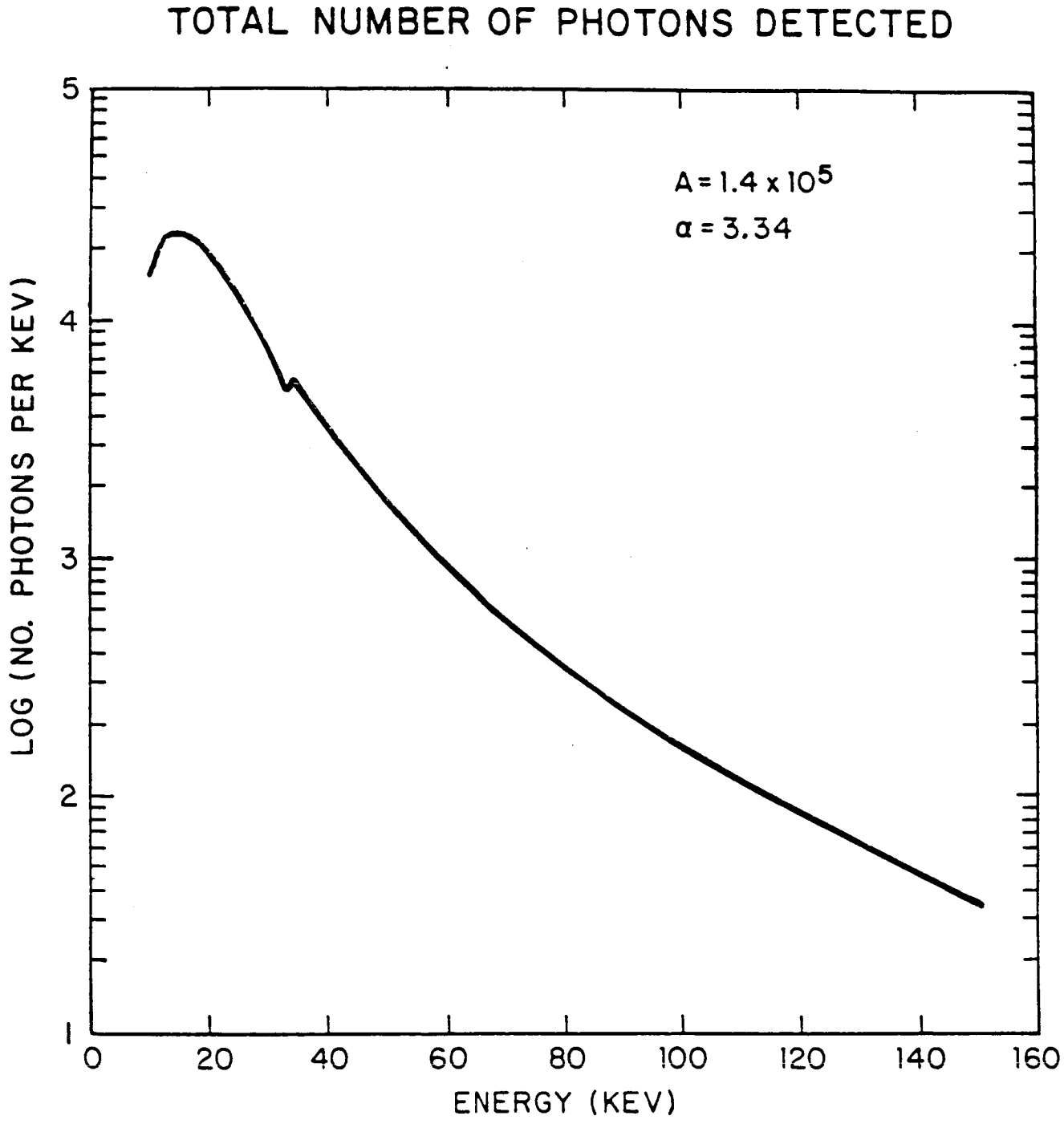
TOTAL NUMBER OF PHOTONS DETECTED
A = 1.4 x 10^5
α = 3.34
LOG (NO. PHOTONS PER KEV)
ENERGY (KEV)
5
4
3
2
1
0
20
40
60
80
100
120
140
160

Figure 8a

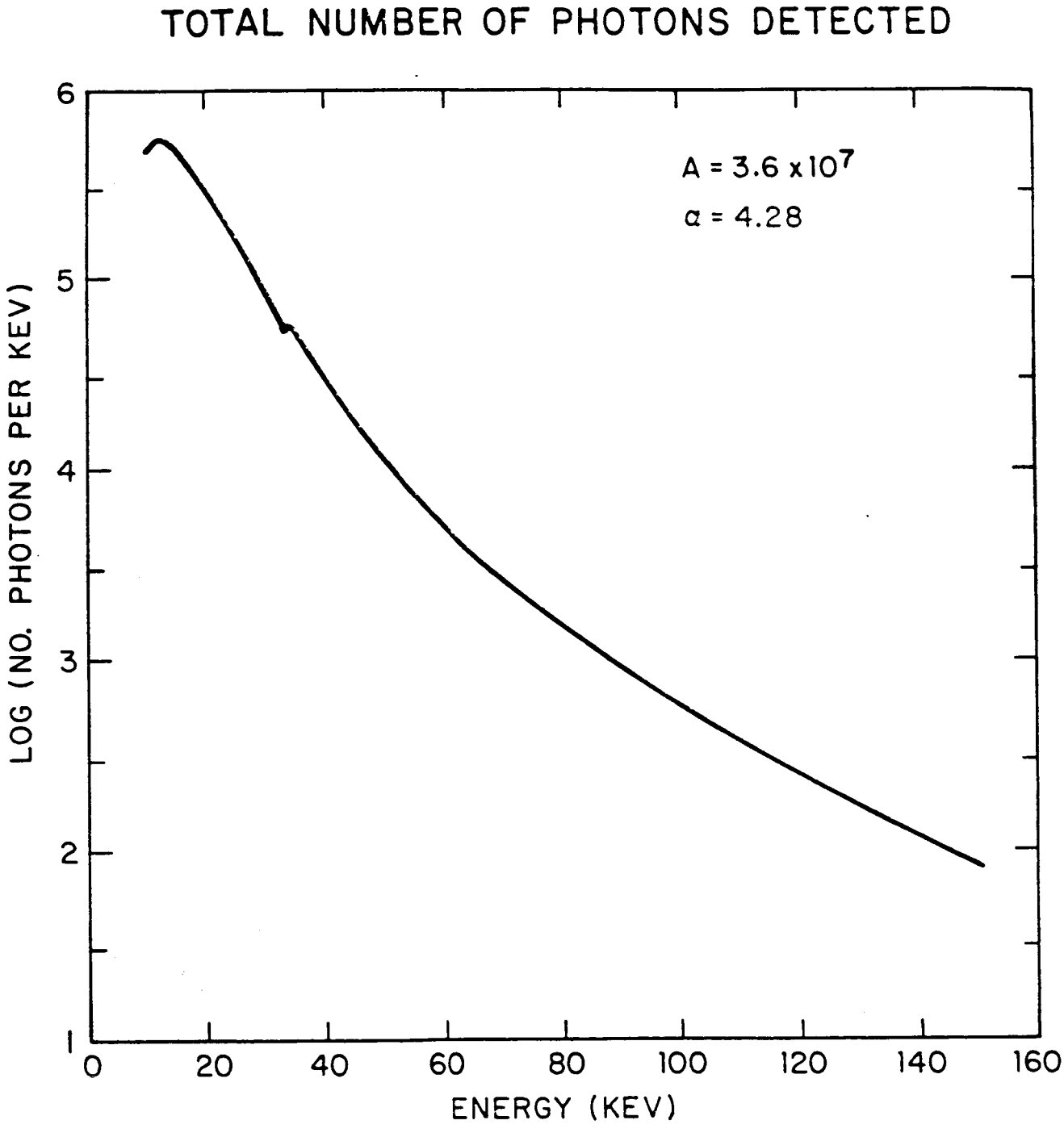
TOTAL NUMBER OF PHOTONS DETECTED
A = 3.6 x 10^7
α = 4.28
LOG (NO. PHOTONS PER KEV)
ENERGY (KEV)
6
5
4
3
2
1
0
20
40
60
80
100
120
140
160

Figure 8b

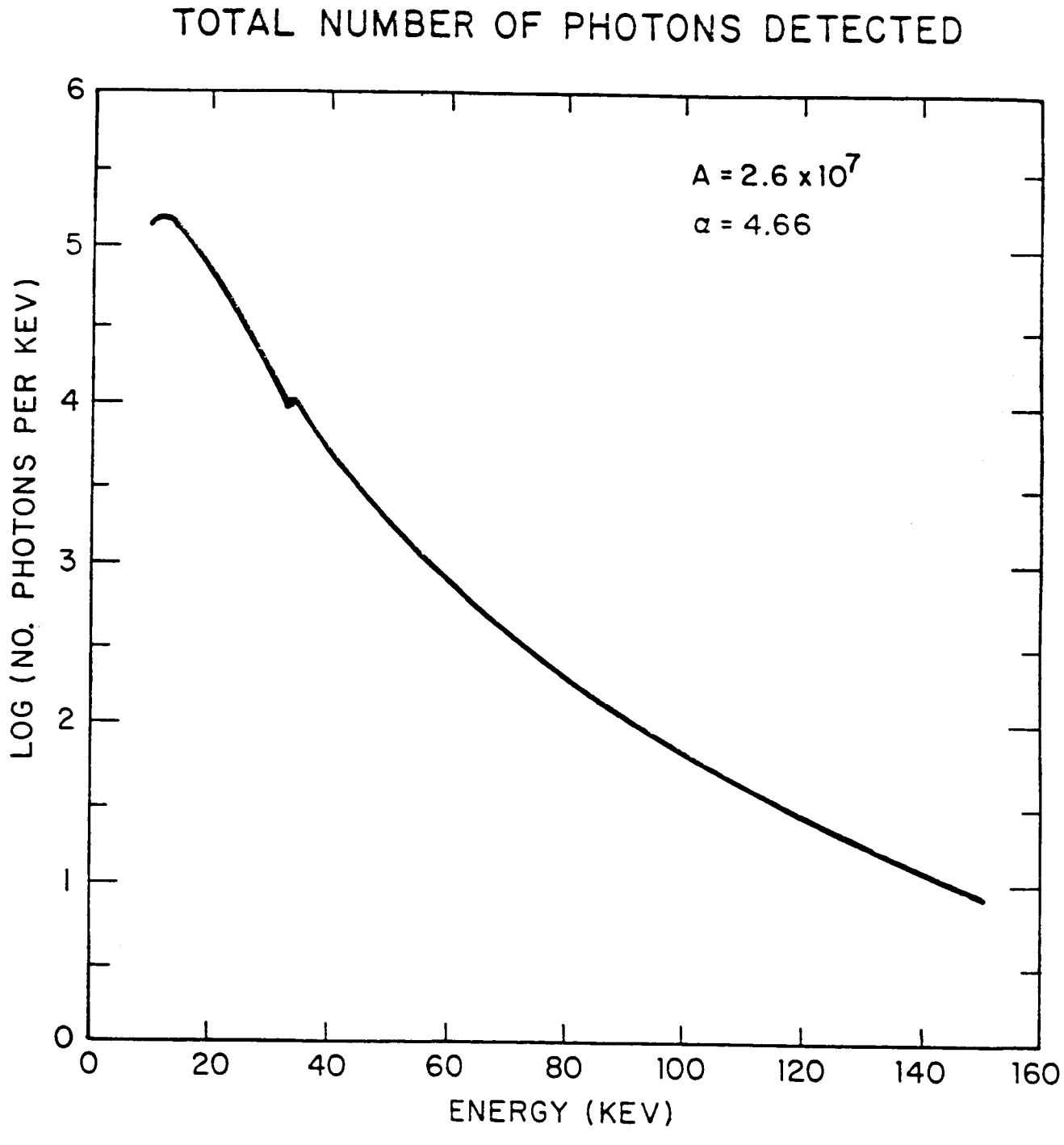
TOTAL NUMBER OF PHOTONS DETECTED
A = 2.6 x 10^7
α = 4.66
LOG (NO. PHOTONS PER KEV)
ENERGY (KEV)
0
1
2
3
4
5
6
0
20
40
60
80
100
120
140
160

Figure 8c

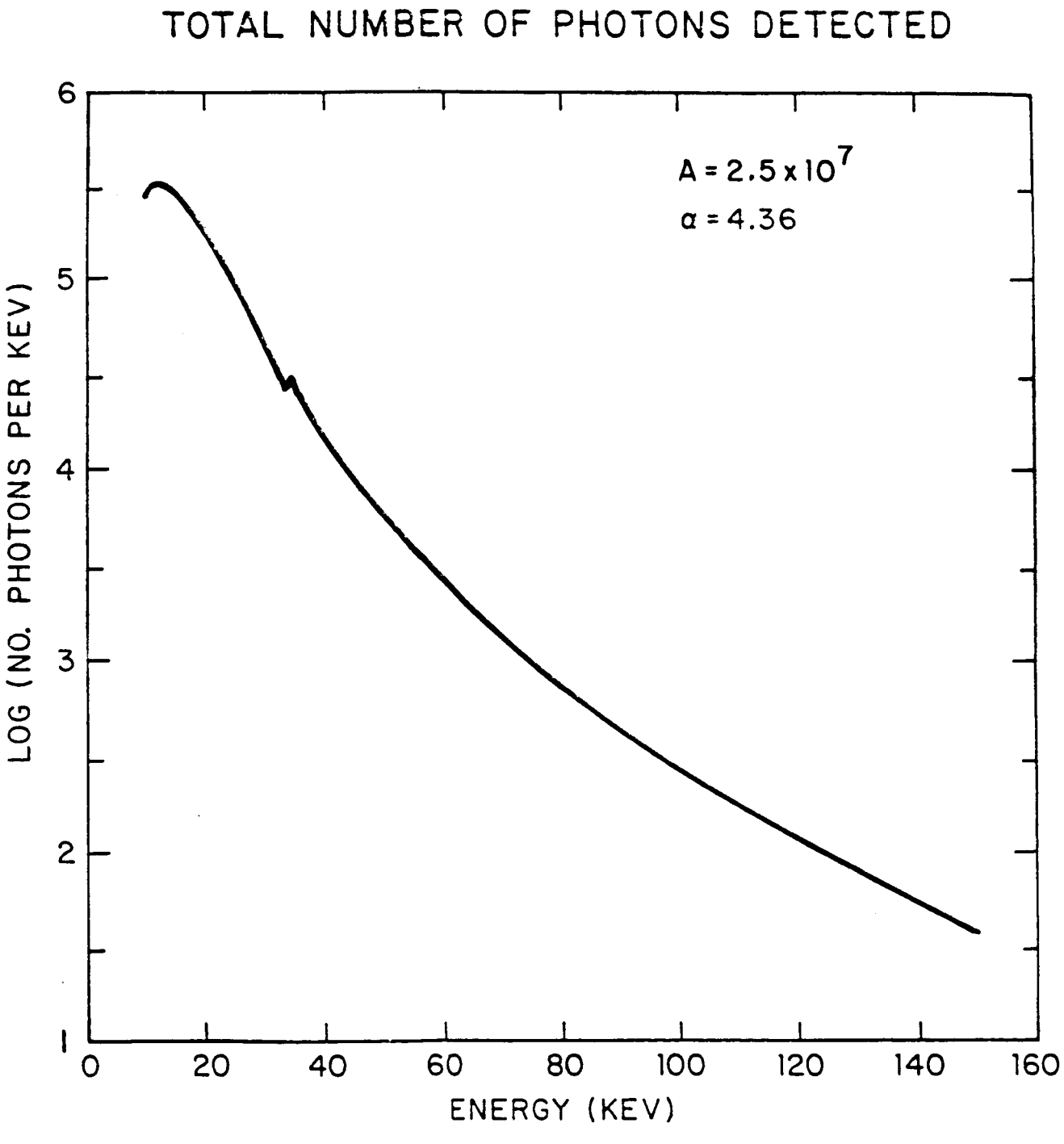
TOTAL NUMBER OF PHOTONS DETECTED
A = 2.5 x 10^7
α = 4.36
LOG (NO. PHOTONS PER KEV)
ENERGY (KEV)
6
5
4
3
2
1
0
20
40
60
80
100
120
140
160

Figure 8d

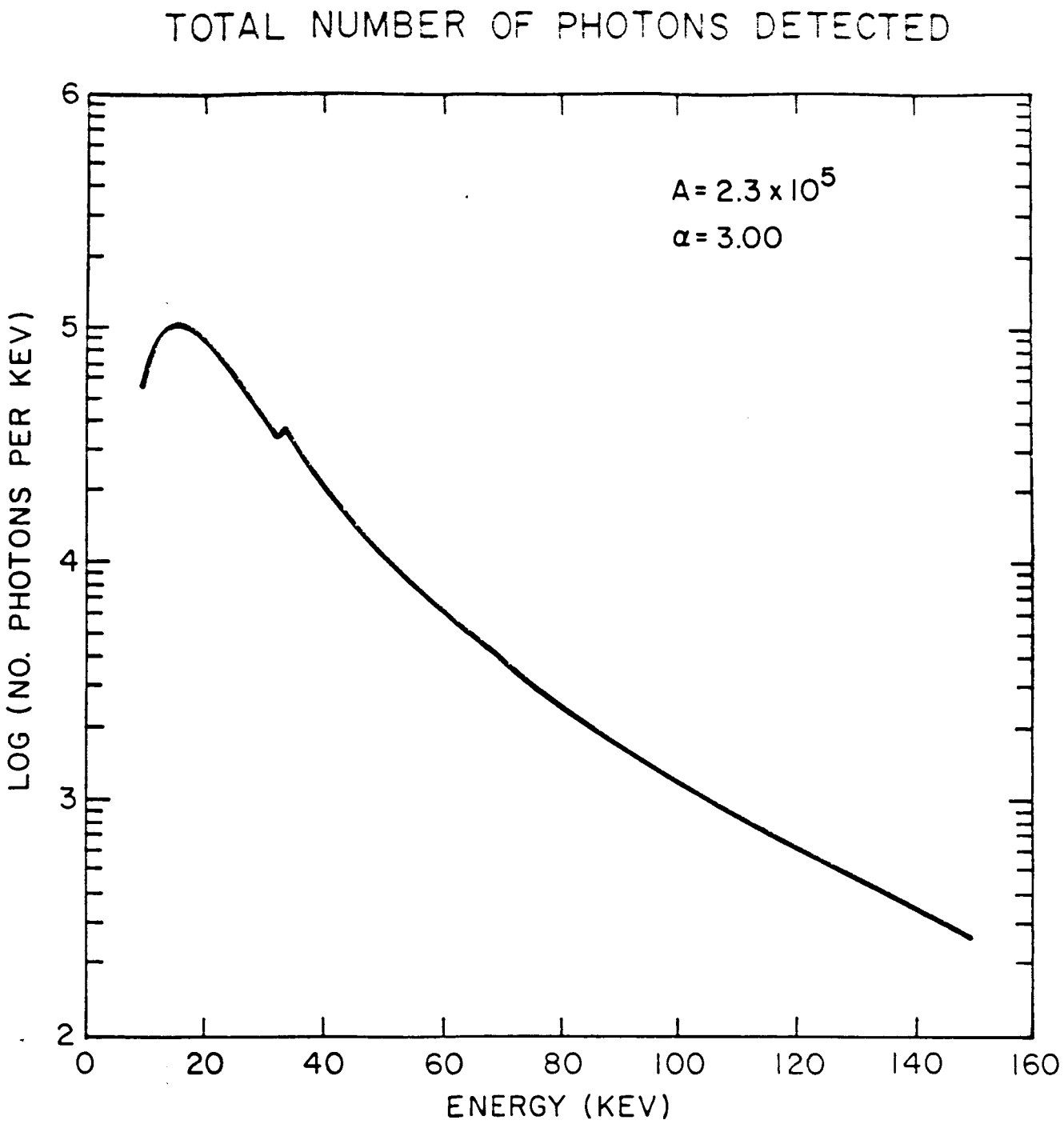
TOTAL NUMBER OF PHOTONS DETECTED
A = 2.3 x 10^5
α = 3.00
LOG (NO. PHOTONS PER KEV)
ENERGY (KEV)
6
5
4
3
2
0
20
40
60
80
100
120
140
160

Figure 8e

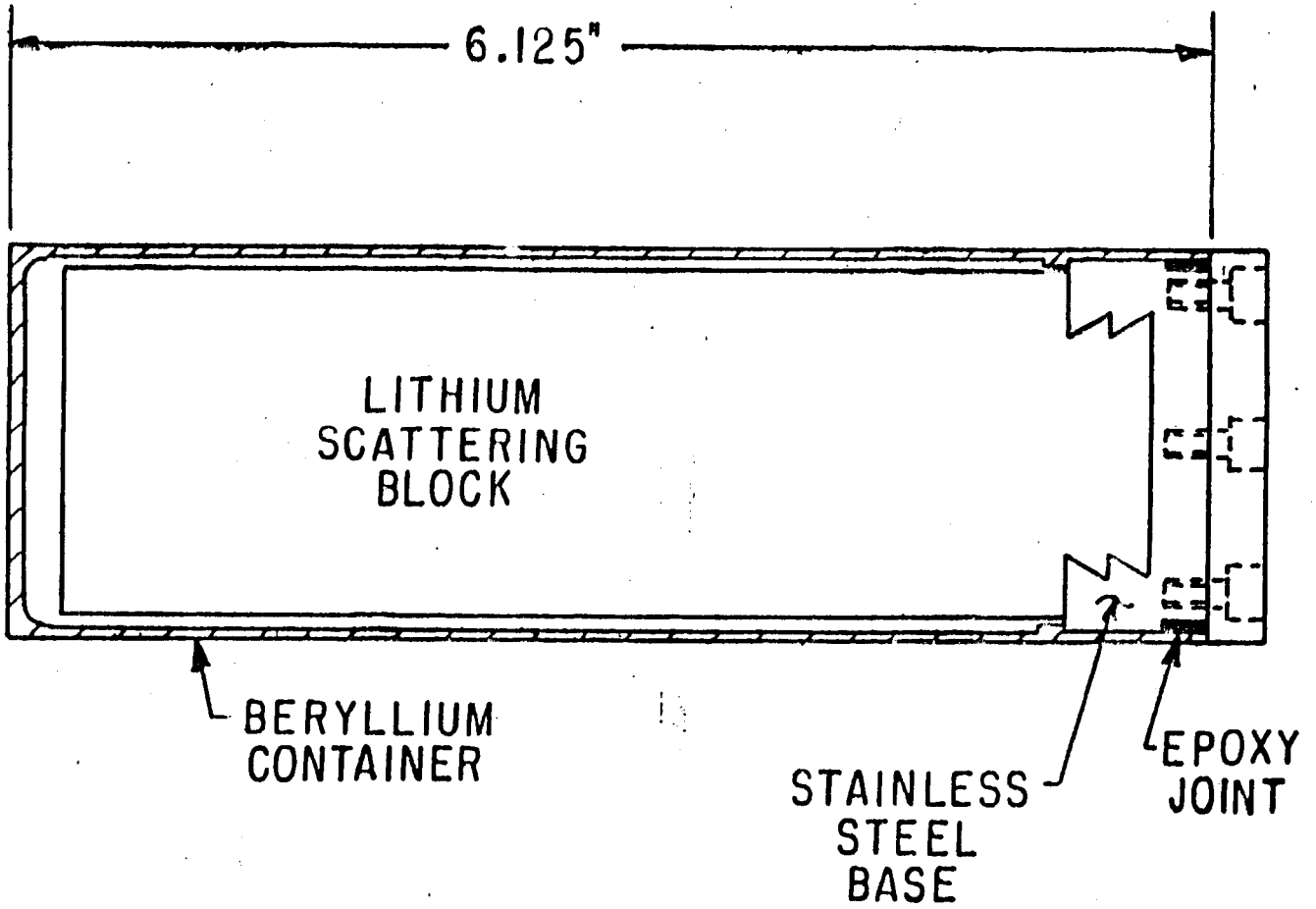
6.125"
LITHIUM
SCATTERING
BLOCK
BERYLLIUM
CONTAINER
STAINLESS
STEEL
BASE
EPOXY
JOINT

Figure 9

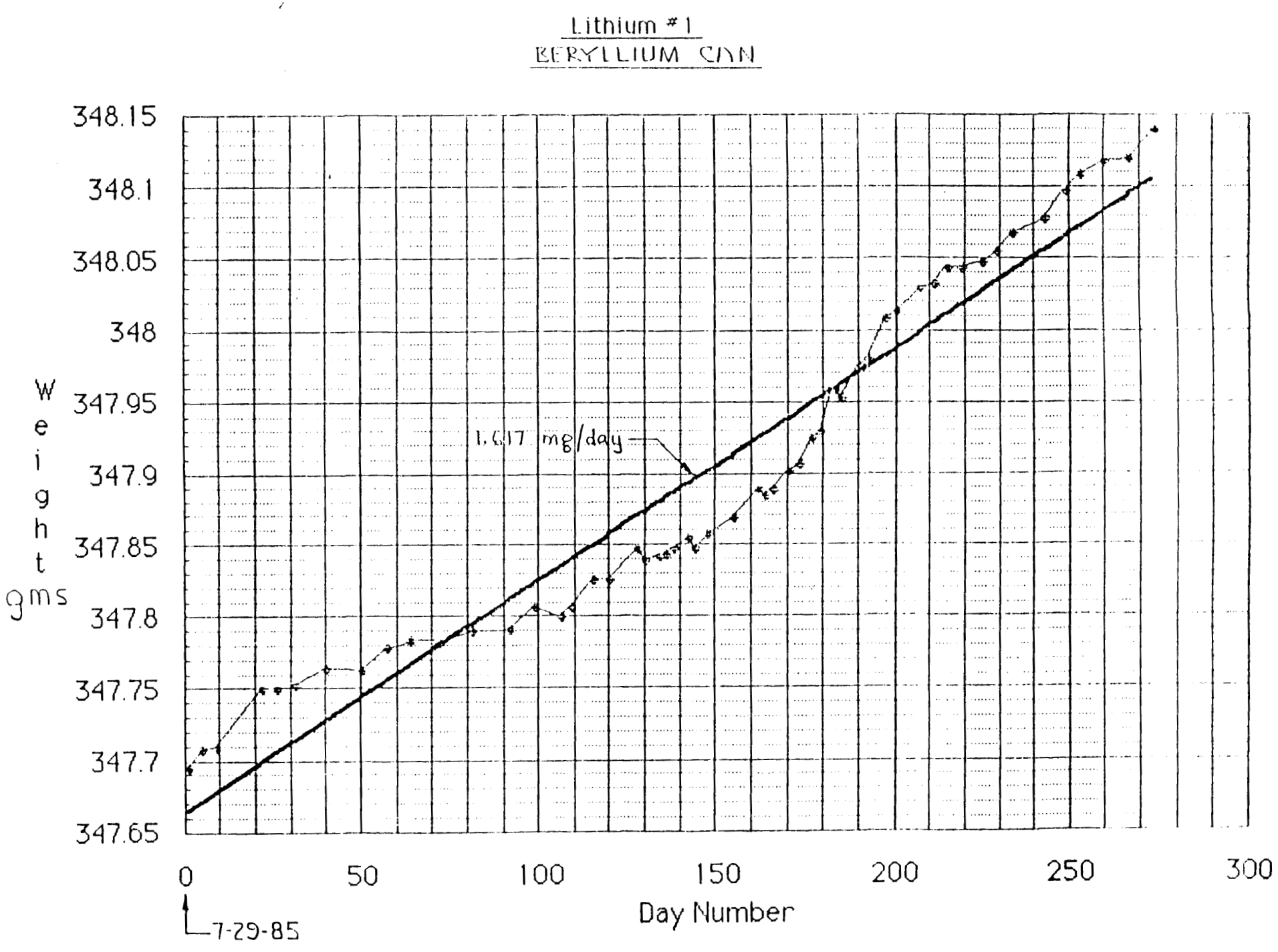
Lithium #1
BERYLLIUM CAN
348.15
348.1
348.05
348
347.95
347.9
347.85
347.8
347.75
347.7
347.65
Weight gms
1.617 mg/day
0
50
100
150
200
250
300
Day Number
7-29-85

Figure 10a

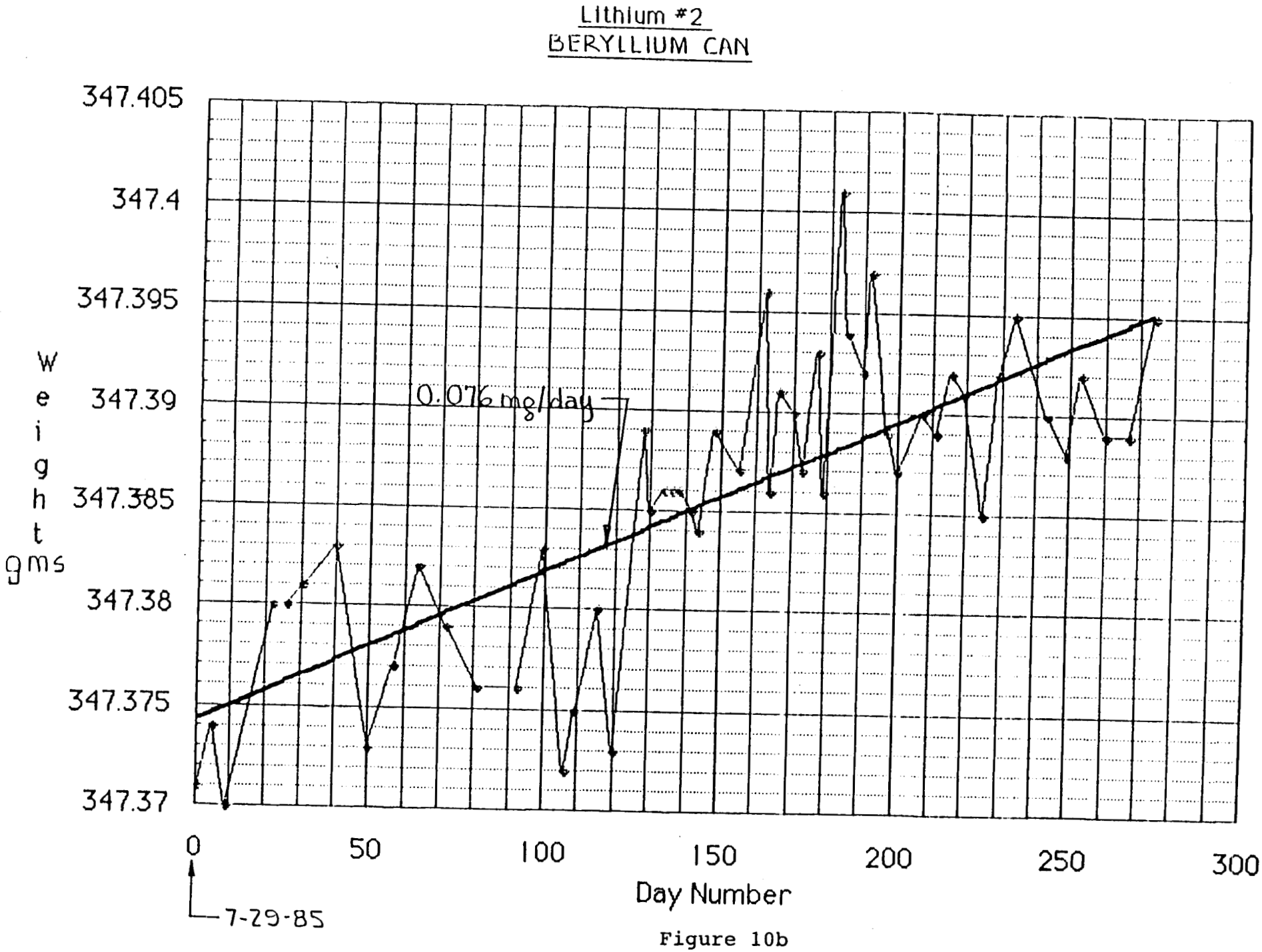
Lithium #2
BERYLLIUM CAN
347.405
347.4
347.395
347.39
347.385
347.38
347.375
347.37
Weight gms
0.076 mg/day
0
50
100
150
200
250
300
Day Number
7-29-85

Figure 10b

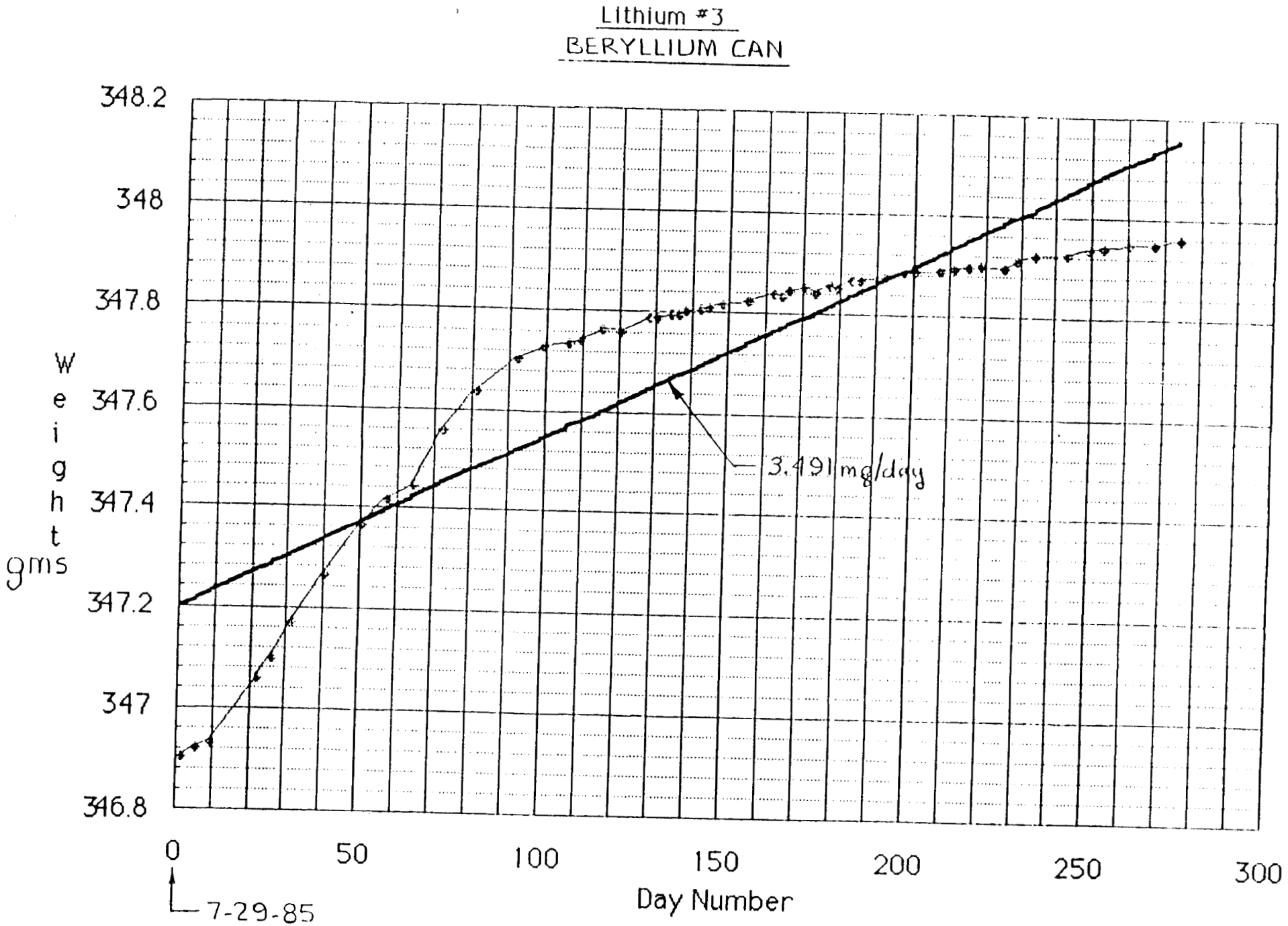
Lithium #3
BERYLLIUM CAN
348.2
348
347.8
347.6
347.4
347.2
347
346.8
Weight gms
3.491 mg/day
0
50
100
150
200
250
300
7-29-85
Day Number

Figure 10c

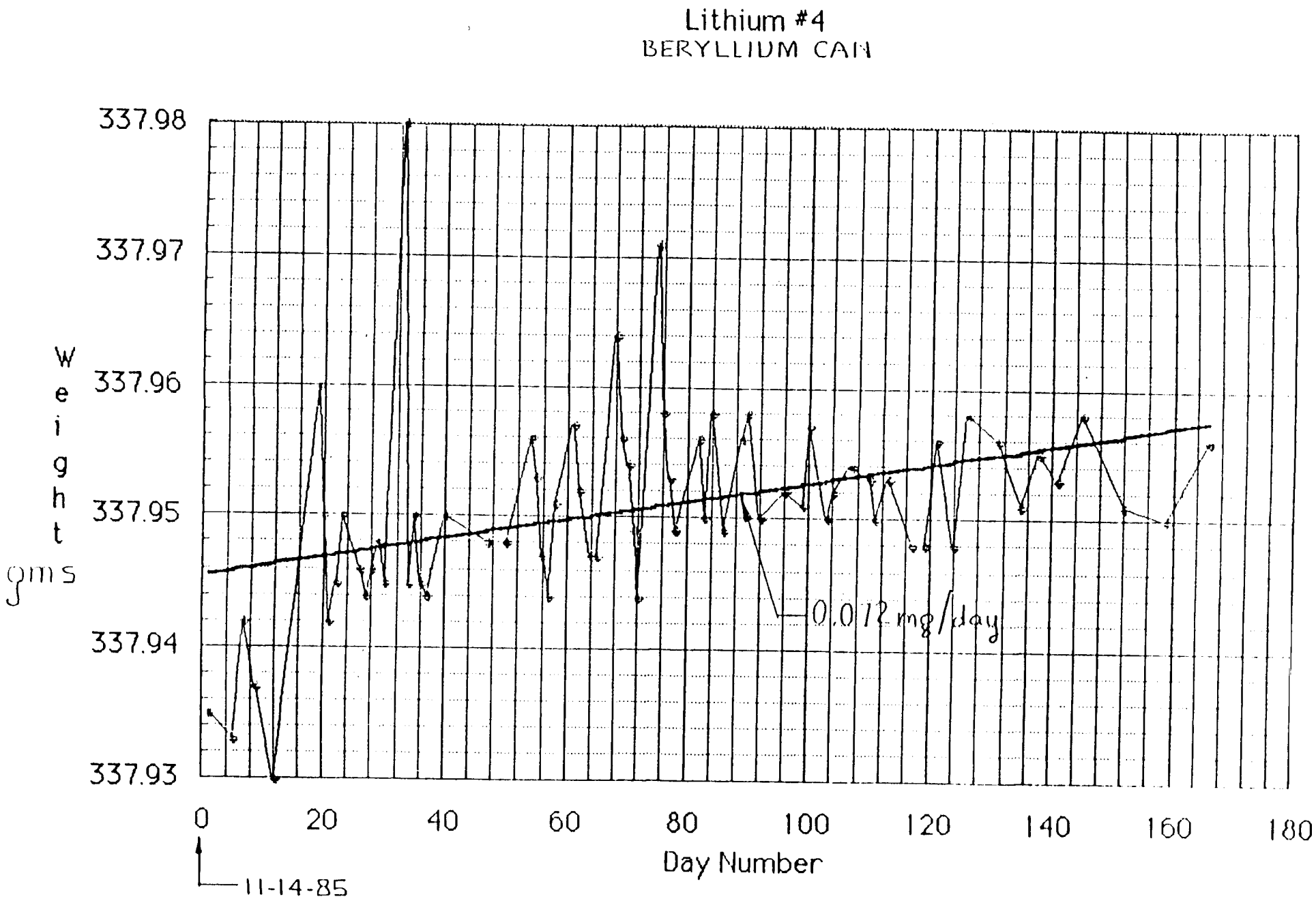
Lithium #4
BERYLLIUM CAN
337.98
337.97
337.96
337.95
337.94
337.93
Weight gms
0.012 mg/day
0
20
40
60
80
100
120
140
160
180
Day Number
11-14-85

Figure 10d

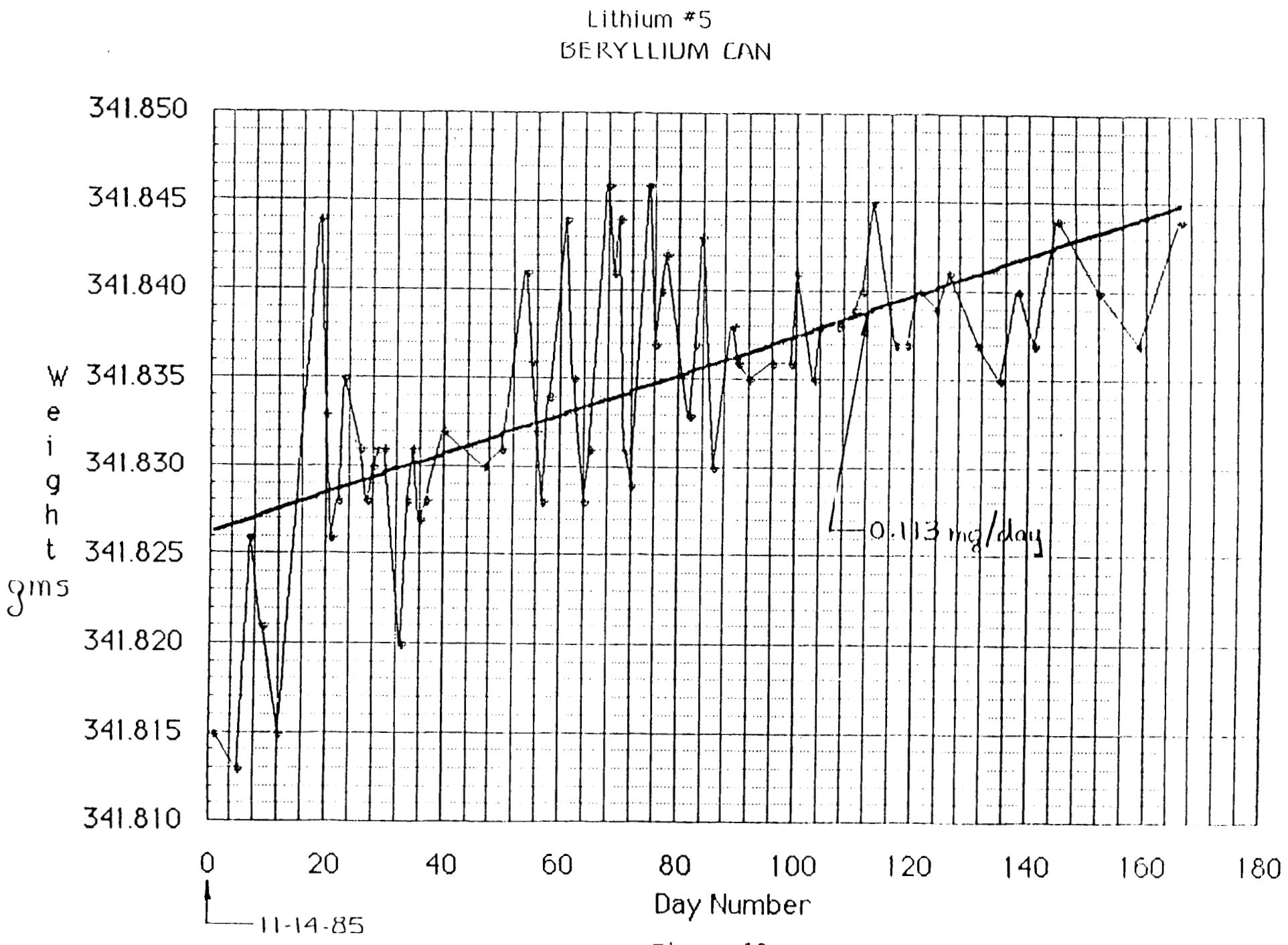
Lithium #5
BERYLLIUM CAN
341.850
341.845
341.840
341.835
341.830
341.825
341.820
341.815
341.810
Weight gms
0.113 mg/day
0
20
40
60
80
100
120
140
160
180
Day Number
11-14-85

Figure 10e

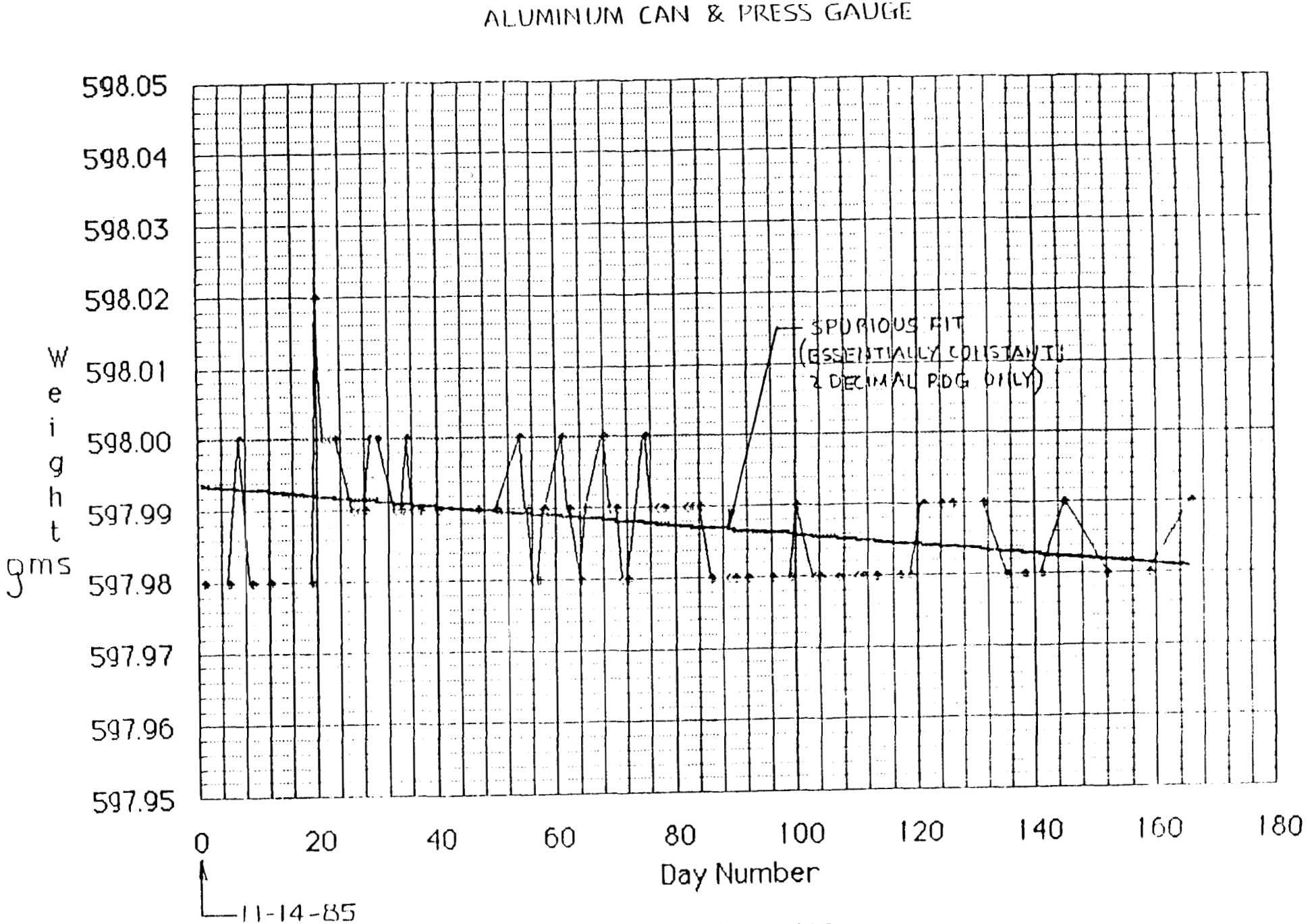
Lithium #6
ALUMINUM CAN & PRESS GAUGE
598.05
598.04
598.03
598.02
598.01
598.00
597.99
597.98
597.97
597.96
597.95
Weight gms
SPURIOUS FIT
(ESSENTIALLY CONSTANT
2 DECIMAL PDG ONLY)
0
20
40
60
80
100
120
140
160
180
Day Number
11-14-85

Figure 10f